Journal of Power Sources 195 (2010) 5896–5901

Contents lists available at ScienceDirect

Journal of Power Sources

journal homepage: www.elsevier.com/locate/jpowsour

Shape-controlled Pd nanostructure catalysts for highly efficient electrochemical power sources

Young-Woo Lee[a], Jae-Kyung Oh[a], Hyun-Su Kim[a], Jin-Kyu Lee[a], Sang-Beom Han[a], Woojin Choi[b], Kyung-Won Park[a,*]

[a] Department of Chemical and Environmental Engineering, Soongsil University, 511 Sangdo-dong, Dongjak-gu, Seoul 156-743, Republic of Korea
[b] Department of Electrical Engineering, Soongsil University, Seoul 156-743, Republic of Korea

ARTICLE INFO

Article history:
Received 6 October 2009
Received in revised form
30 November 2009
Accepted 2 December 2009
Available online 11 December 2009

Keywords:
Shape-control
Pd catalyst
Formic acid oxidation
Iodide reduction

ABSTRACT

We report polygonal Pd catalysts on carbon black synthesized by means of polyol process in the presence of poly(vinyl pyrrolidone) and NO_3^- ion. We find that the polygonal Pd/C has dominant {1 1 1} facets observed by X-ray diffraction method and transmission electron microscopy analysis. The current density for formic acid electrooxidation of polygonal Pd/C (1.908 mA cm^{-2}) with controlled surface structures such as dominant {1 1 1} facets is much higher than Pd/C (0.478 mA cm^{-2}) at 0 V. Furthermore, the polygonal Pd/C with controlled surface structures shows much improved performances in dye-sensitized solar cells (DSSCs) due to its highly thermal stability and enhanced catalytic activity for iodide reduction.

1. Introduction

Platinum has been of major interest as a catalyst for electrochemical power sources such as direct formic acid fuel cells (DFAFCs) and dye-sensitized solar cells (DSSCs) due to its excellent activity and stability in comparison with other metallic catalysts. Typically, Pt and Pt-based metallic structures have been utilized as electrocatalysts for formic acid electrooxidation in DFAFCs and efficient counter electrodes for iodide reduction in DSSCs [1–8]. In DSSCs, many efforts have been made to improve efficiency and long-term stability in the anode [9,10], whereas only few studies of the cathode for the iodide reduction in DSSCs have been reported [11,12]. However, since Pt is highly expensive for mass production, the catalyst for electrochemical power sources should be replaced with a potential candidate with high energy conversion efficiency and low cost [13–15].

In particular, metallic nanostructures can have significantly enhanced catalytic reaction rates over those of bulk materials [16,17]. In metallic electrodes for DFAFCs and DSSCs, crucial factors affecting catalytic activity are size, structure, and shape of catalysts. Recently, it has been reported that nanostructure catalysts could be controlled by electrodeposition in the electrochemical process for preparation of metal nanoparticles [4,18]. Furthermore, to increase activity of metallic nanostructure catalysts, there have been many efforts to manipulate structure and shape of nanoparticles during synthetic process [19–23].

In this work, we synthesized polygonal Pd on Vulcan XC-72R using a polyol process in the presence of poly (vinyl pyrrolidone) and NO_3^- ion. The crystal structure of the catalyst was confirmed by X-ray diffraction analysis and field-emission transmission electron microscopy. To characterize photoelectrochemical properties and cell performances in DFAFCs and the DSSCs, cyclic voltammograms (CVs) and current–voltage curves were obtained using synthesized catalysts compared to conventional catalysts.

2. Experimental

The carbon black (Vulcan XC-72R) supported Pd (20 wt%) catalyst was prepared by reducing Pd salt in ethylene glycol (EG) solution. A solution of metal salt of 2 mM Na_2PdCl_4 and slower reduction additives such as 10 mM $NaNO_3$ and 20 μM $FeCl_3$ was dissolved in 50 ml of EG with 50 mg poly(vinyl pyrrolidone) (PVP, MW = 29,000) and Vulcan XC-72R treated in 5 M HCl solution at 50 °C for 12 h [30,31]. All chemicals used were of analytical grade. The solution was raised by 5 °C min^{-1} and was kept for 3 h at 250 °C until Na_2PdCl_4 was completely reduced by EG. The resulting colloid solution was cooled at room temperature and then washed with water and ethanol several times to remove ethylene glycol and excess PVP.

* Corresponding author. Tel.: +82 2 820 063; fax: +82 2 812 5378.
E-mail address: kwpark@ssu.ac.kr (K.-W. Park).

0378-7753/$ – see front matter © 2009 Elsevier B.V. All rights reserved.
doi:10.1016/j.jpowsour.2009.12.013

X-ray diffraction (XRD) analysis was carried out using Rigaku X-ray diffractometer with Cu Kα (λ = 0.15418 nm) source with a Ni filter operated at 40 kV and 100 mA. The 2θ angular scan from 20° to 80° was explored at a scan rate of 5° min^{-1}. For all the XRD measurement, the resolution in the scans was kept at 0.02°. The ratio of (1 1 1) to (200) of the samples was measured using D/MAX-2000/PC software (Rigaku Co.), which the background was adjusted by means of Sonnevelt–Visser's method. The morphology, structure, and size distribution of the catalysts were characterized by field-emission transmission electron microscopy (FE-TEM) using a Tecnai G2 F30 system operating at 300 kV. The TEM samples were prepared by placing a drop of catalyst suspension dispersed in an ethanol on a carbon-coated copper grid. The average particle size was calculated by measuring the size of all the polygonal Pd NPs with total number of 70–80. The electrochemical properties of the catalysts were measured in a three-electrode cell at room temperature using a potentiostat (Eco Chemie, AUTOLAB). A Pt wire and Ag/AgCl (in saturated KCl) were used as a counter and reference electrode, respectively. The glassy carbon electrode as a working electrode was polished with 1, 0.3, and 0.05 μm Al_2O_3 paste and then washed in deionized water. The catalyst ink was prepared by ultrasonically dispersing catalyst powders in an appropriate amount of Millipore water. The catalyst ink was pipetted onto a glassy carbon working electrode. After drying in 50 °C oven, the loading amount of metal catalyst was identical with 20 μg cm^{-2}. The cyclic voltammograms (CVs) of the electrocatalysts for formic acid electrooxidation were obtained from −0.2 to +1.0 V in each 0.1 M $HClO_4$ and 0.1 M $HClO_4$ + 2 M formic acid. In order to evaluate the electrocatalytic activity toward iodide reduction, the CVs were obtained from −0.2 to +1.3 V in the solution consisting of 0.1 M $LiClO_4$ as supporting electrolyte and 10 mM LiI and 1 mM I_2 as redox couple in acetonitrile solvent.

To prepare counter electrodes for iodide reduction in DSSCs, the paste was prepared using 50 mg powder mixed with 0.09 ml acetic acid, 0.36 ml distilled ion water, 9.1 ml ethanol, 0.25 g ethyl cellulose, and 1.78 ml terpineol, and then evaporated at 80 °C for 20 min. The prepared paste was coated on the FTO glass (F-doped tin oxide, 12 ohm/sq) by doctor blade method and annealed at 500 °C for 30 min in N_2 atmosphere. For photoanodes, the TiO_2 paste (Solaronix, Ti-nanoxide HT/SP) was deposited on the FTO glass by using doctor blade technique. The films were annealed at 450 °C for 1 h in air atmosphere and soaked in an anhydrous ethanol solution containing 5×10^{-4} M Ru535 (Solaronix, N3 dye) for 24 h. The dye-absorbed TiO_2 film used as working electrodes in two-electrode sandwich cells with effective areas of 0.16 cm^2 and the inner space was filled with a liquid electrolyte containing 0.5 M LiI and 0.05 M I_2 as a redox mediator. Photocurrent measurements were carried out using a 500 W Xe lamp (XIL model 05A50KS) simulated AM 1.5 solar irradiance with the intensity of 100 mW cm^{-2}, which was adjusted using a NREL fabricated Si reference solar cell.

3. Results and discussion

Fig. 1 shows XRD patterns of synthesized Pd on Vulcan XC-72R compared to those of commercial Pt/C (E-TEK, Co.) and commercial Pd/C (E-TEK, Co.). The diffraction peaks at 40.1°, 46.6°, and 68.1° correspond to (1 1 1), (2 0 0), and (2 2 0) plane, respectively, of face centered cubic (fcc) structure of Pd metallic phase. The broad peak around 25° was associated with (0 0 2) plane of the Vulcan XC-72R carbon support. The intensity ratio of (1 1 1) to (2 0 0) of synthesized Pd/C, commercial Pt/C, and commercial Pd/C is 3.27, 2.99, and 2.74, respectively. The full-width half-maximum (FWHM) calculated by Scherer equation in (2 2 0) planes of the polygonal Pd/C, Pt/C, and Pd/C is 0.83°, 2.40°, and 2.12°, respectively. This suggests that the

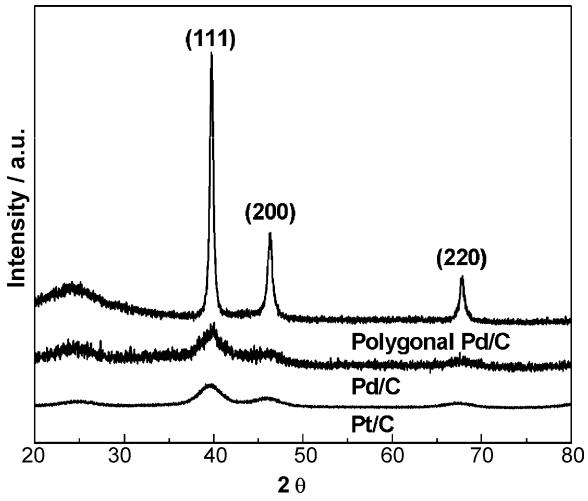

Fig. 1. XRD patterns of polygonal Pd/C catalyst synthesized by polyol process, Pt/C (E-TEK), and Pd/C (E-TEK).

polygonal Pd/C shows highly dominant (1 1 1) plane compared to Pt/C and Pd/C.

Fig. 2 shows comparison of TEM images of the polygonal Pd/C, Pt/C, and Pd/C before and after annealing at 500 °C, respectively. In Fig. 2(a), the average particle size of polygonal Pd nanoparticles such as dodecahedron, decahedron, triangular, and hexagonal plates is ∼34.37 nm. The polygonal Pd/C represents the {1 1 1} facets with *d*-spacing of 0.229 nm of Pd metallic phase with a face centered cubic (fcc) crystal structure. It is evident that the polygonal Pd nanoparticles with dominant {1 1 1} facets are formed during the polyol process, which the {1 1 1} facets have the lowest total free energy by maximizing the surface coverage. As shown in Fig. 2(b), the polygonal Pd/C shows highly thermal stability for angular shapes without any serious agglomeration after annealing at 500 °C. On the other hand, Pt/C (Fig. 4(d)) and Pd/C (Fig. 4(f)) show an agglomeration between nanoparticles and increased particle size due to degradation during annealing at 500 °C. This suggests that highly thermal stability of the polygonal Pd/C is superior to that of Pt/C and Pd/C.

In Fig. 3(a), the CVs of the catalysts are obtained in 0.1 M $HClO_4$ between −0.2 and 1.0 V. The electrochemical active surface area (EASA) of the catalysts were measured by integrating hydrogen adsorption and desorption region assuming 210 μC cm^{-2} of Pt and 95 μC cm^{-2} of Pd. The EASAs are 7.12, 30.33, and 22.62 m^2 g^{-1} for the polygonal Pd/C, Pt/C, and Pd/C, respectively. The CVs of Pd/C catalysts for formic acid oxidation are shown in Fig. 3(b). In comparison of the CVs, the polygonal Pd/C shows more negative peak potential (0.195 V) for oxidation than 0.653 V of Pd/C. The current density of polygonal Pd/C (1.908 mA cm^{-2}) is much higher than Pd/C (0.478 mA cm^{-2}) at 0 V. Recently, Hoshi et al. [24] and Baldauf and Kolb [25] reported that {1 1 1} facets of Pd represented particularly faster oxidation potential peaks than other facets of Pd/C as shown in our data. Thus, this suggests that the polygonal Pd/C with controlled surface structures such as dominant {1 1 1} facets shows improved electrocatalytic activity for formic acid oxidation in comparison with Pd/C.

Fig. 4 shows CVs of I_3^-/I^- system for the polygonal Pd/C, Pt/C, and Pd/C electrodes before and after annealing at 500 °C. In the CVs with I_3^-/I^- redox peaks, the more positive pair is assigned to redox reaction of Eq. (1) and negative one is assigned to redox reaction of Eq. (2). However, in actual, the I_3^-/I^- redox peaks of all catalysts according to Eq. (2) become significant redox reaction between electrolytes and counter electrodes in the DSSCs.

$$3I_2 + 2e^- \leftrightarrow 2I_3^- \quad (1)$$

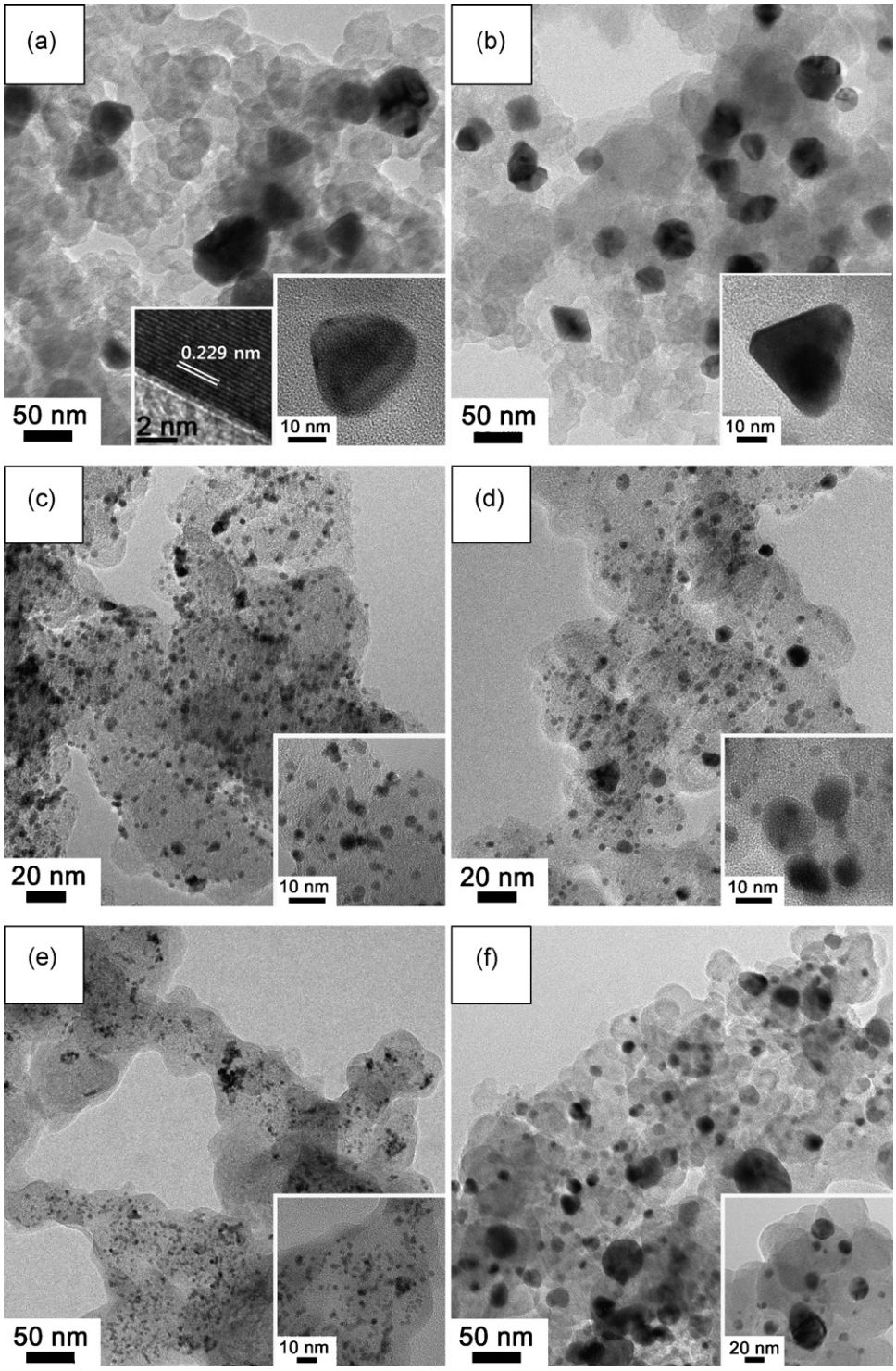

Fig. 2. TEM images of polygonal Pd/C (a and b), Pt/C (c and d), and Pd/C (e and f) before and after annealing at 500 °C, respectively. (The inset indicates a high-resolution image of the catalyst.)

$$I_3^- + 2e^- \leftrightarrow 3I^- \quad (2)$$

$$\text{Anodic peak}\,(\sim 0.3\,\text{V}) : 3I^- \rightarrow I_3^- + 2e^- \quad (2\text{-}1)$$

$$\text{Cathodic peak}\,(\sim 0.1\,\text{V}) : I_3^- + 2e^- \rightarrow 3I^- \quad (2\text{-}2)$$

In general, electrons are usually injected to photo-oxidized dye from I^- ions in the electrolyte (Eq. (2-1)), and the produced I_3^- ions are reduced on the counter electrode (Eq. (2-2)) in the DSSCs. As shown in Fig. 4(d), the polygonal Pd/C after annealing treatment at 500 °C shows a reduction current similar to Pt/C and 1.48 times higher than Pd/C at I_3^- reduction potential (A). It is likely that improved electrochemical properties of the polygonal Pd/C result from controlled surface structures in spite of much smaller EASA of the polygonal Pd/C than other electrodes (Fig. 3(a)). Fig. 5 illustrates a relation between all the peak currents at reduction potential of I_3^- (A in the Fig. 4(d)) as a function of a square root of scan rate. The linear relationship with various scan rates means the diffusion limitation of the redox reaction, which can be related with the transport

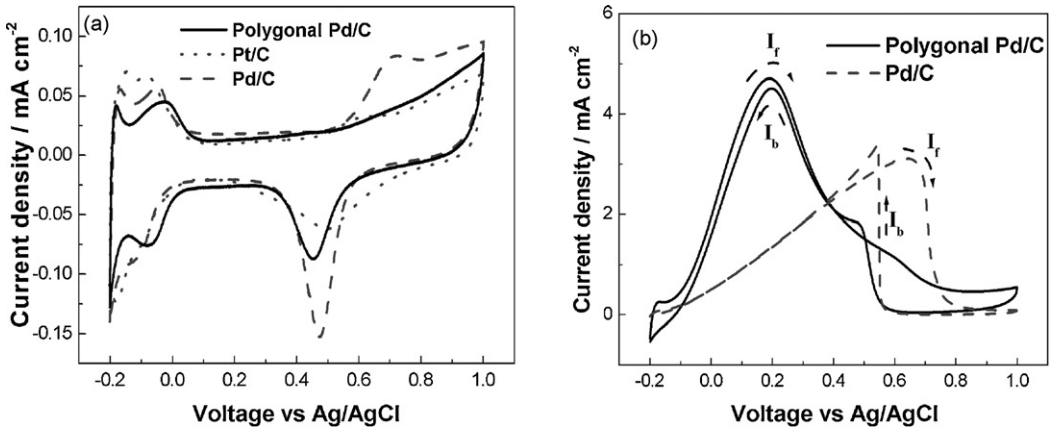

Fig. 3. (a) CVs of polygonal Pd/C, Pt/C, and Pd/C catalysts in 0.1 M $HClO_4$ with a scan rate of 50 mV s^{-1}. (b) CVs of polygonal Pd/C and Pd/C catalysts in 0.1 M $HClO_4$ + 2 M formic acid with a scan rate of 50 mV s^{-1}. The loading amount of metal catalyst on the electrode is 20 μg cm^{-2}.

of iodide species [26]. The reduction rate of I_3^- on counter electorde should be explained by the diffusion coefficient (D_a) [27,28]. The diffusion coefficient was calculated using Randles–Sevcik equation of $I_p = (2.69 \times 10^5)n^{3/2}AD_a^{1/2}C_0^*v^{1/2}$, where I_P is current density, n is the number of electrons, A is the area of the electrode, C_0^* is the concentration in bulk solution, and v is the scan rate involved in the reaction. The slopes of linear curves for the polygonal Pd/C, Pt/C, and Pd/C are −0.0081, −0.0065, and −0.0072, respectively. The diffusion coefficients calculated from the slopes are 7.08×10^{-6}, 4.56×10^{-6}, and 5.60×10^{-6} cm^2 s^{-1} for the polygonal Pd/C, Pt/C, and Pd/C, respectively. This means that despite smaller EASA of the polygonal Pd/C than other electrodes in Fig. 3(a), the polygonal Pd/C has higher diffusion coefficient as a counter electrode in dye-sensitized solar cells.

To analyze and compare photoelectrochemical properties in dye-sensitized solar cells, as shown in Fig. 6(a), photocurrent–voltage curves were obtained using the polygonal Pd/C, Pt/C, and Pd/C as counter electrodes. The short circuit

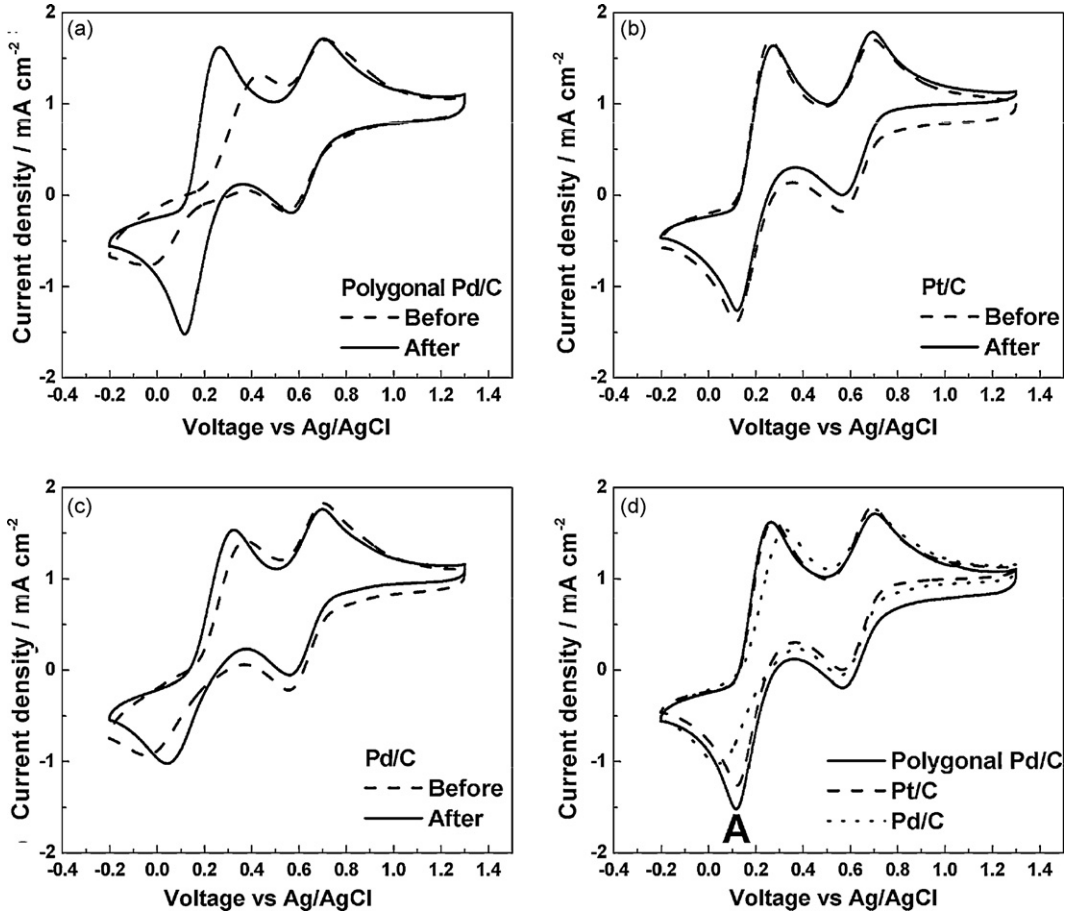

Fig. 4. CVs of (a) polygonal Pd/C, (b) Pt/C, and (c) Pd/C before and after annealing at 500 °C, respectively, in acetonitrile solution of 10 mM LiI, 1 mM I_2, and 0.1 M $LiClO_4$ with a scan rate of 50 mV s^{-1}. (d) CVs of the electrodes after annealing at 500 °C.

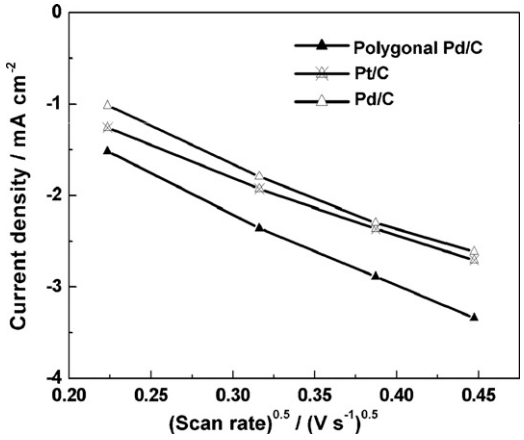

Fig. 5. Redox peak currents of I_3^- at reduction potential (A in Fig. 4(d)) as a function of scan rates using polygonal Pd/C, Pt/C, and Pd/C catalysts.

current density (J_{sc}), open circuit voltage (V_{oc}), fill factor (FF), and efficiency (η) were summarized in Table 1. It is considered that since the polygonal Pd/C despite much smaller EASA has controlled surface structures such as dominant {1 1 1} facets, the polygonal Pd/C shows higher cell efficiency than Pd/C and slightly lower than Pt/C. Furthermore, in Fig. 6(b), dark current density of the polygonal Pd/C is similar to Pt/C and higher than Pd/C. This means that high current of the polygonal Pd/C as a counter

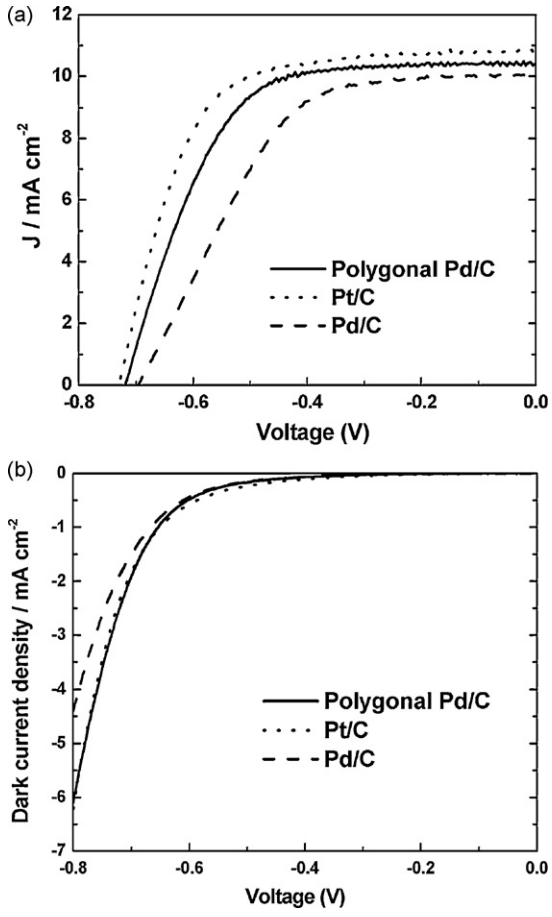

Fig. 6. (a) Photocurrent–voltage curves and (b) dark current–voltage curves in dye-sensitized solar cells using polygonal Pd/C, Pt/C, and Pd/C as counter electrodes.

Table 1
Comparison of cell performance of dye-sensitized solar cells (DSSCs) using polygonal Pd/C, Pt/C, and Pd/C as counter electrodes. The J_{sc}, V_{oc}, FF, and η are short circuit current density, open circuit voltage, fill factor, and efficiency in DSSCs, respectively.

Samples	V_{oc} (V)	J_{sc} (mA cm^{-2})	FF (%)	η (%)
Polygonal Pd	0.72	10.47	62.6	4.71
Pt/C	0.73	10.88	66	5.22
Pd/C	0.69	10.09	54.4	3.79

electrode results from such an improved catalytic activity for iodide reduction [29]. Thus, by combing electrochemical data and structural analysis, it is concluded that the polygonal Pd/C can be a promising candidate for the counter electrode in DSSCs.

4. Conclusions

The polygonal Pd catalysts on carbon black were successfully synthesized by means of polyol process. The controlled surface structure such as dominant {1 1 1} facets in the polygonal Pd/C could result in an excellent catalytic activity for formic acid electrooxidation in comparison with Pd/C. Furthermore, the synthesized polygonal Pd/C has highly thermal stability and improved iodide reduction in spite of smaller EASAs than Pt/C and Pd/C. Thus, we suggest that the structure-controlled Pd nanostructure electrode can be a promising catalyst for formic acid electrooxidation and iodide reduction.

Acknowledgments

This work was supported by New & Renewable Energy R&D Program (2008-N-FC08-P-01-3-030), the Human Resource Training Project for Strategic Technology, and Manpower Development Program for Energy & Resources of the Ministry of Knowledge and Economy, Republic of Korea.

References

[1] E. Antolini, F. Colmati, E.R. Gonzalez, Electrochem. Commun. 9 (2007) 398–404.
[2] Y.-J. Song, S.-B. Han, J.-M. Lee, K.-W. Park, J. Alloy. Compd 473 (2009) 516–520.
[3] W.J. Zhou, B. Zhou, W.Z. Li, Z.H. Zhou, S.Q. Song, G.Q. Sun, Q. Xin, S. Douvartzides, M. Goula, P. Tsiakaras, J. Power Sources 126 (2004) 16–22.
[4] Y.-J. Song, J.-K. Oh, K.-W. Park, Nanotechnology 19 (2008), 355602 (6PP).
[5] X. Fang, T. Ma, G. Guan, M. Akiyama, T. Kida, E. Abe, J. Electroanal. Chem. 570 (2004) 257–263.
[6] P. Li, J. Wu, J. Lin, M. Huang, Y. Huang, Q. Li, Sol. Energy 83 (2009) 845–849.
[7] B.C.H. Steele, A. Heinzel, Nature 414 (2001) 345–352.
[8] Y.-W. Rhee, S.Y. Ha, R.I. Masel, J. Power Sources 117 (2003) 35–38.
[9] S.G. Chen, S. Chappel, Y. Diamant, A. Zaban, Chem. Mater. 13 (2001) 4629–4634.
[10] S. Hore, P. Nitz, C. Vetter, C. Prahl, M. Niggemann, R. Kern, Chem. Commun. (2005) 2011–2013.
[11] Y. Saito, W. Kubo, T. Kitamura, Y. Wada, S. Yanagida, J. Photochem. Photobiol. A-Chem. 164 (2004) 153–157.
[12] X. Fang, T. Ma, G. Guan, M. Akiyama, E. Abe, J. Photochem. Photobiol. A-Chem. 164 (2004) 179–182.
[13] V. Mazumder, S. Sun, J. Am. Chem. Soc. 131 (2009) 4588–4589.
[14] W. Zhou, J.Y. Lee, J. Phys. Chem. C 112 (2008) 3789–3793.
[15] R. Wang, S. Liao, S. Ji, J. Power Sources 180 (2008) 205–208.
[16] S.-B. Han, Y.-J. Song, J.-M. Lee, J.-Y. Kim, K.-W. Park, Electrochem. Commun. 10 (2008) 1044–1047.
[17] C. Burda, X. Chen, R. Narayanan, M.A. El-Sayed, Chem. Rev. 105 (2005) 1025–1102.
[18] S.-S. Kim, Y.-C. Nah, Y.-Y. Noh, J. Jo, D.-Y. Kim, Electrochim. Acta 51 (2006) 3814–3819.
[19] Y. Xiong, J. Chen, B. Wiley, Y. Xia, Y. Yin, Z.-Y. Li, Nano Lett. 5 (2005) 1237–1242.
[20] Y. Xiong, J. Chen, B. Wiley, Y. Xia, S. Aloni, Y. Yin, J. Am. Chem. Soc. 127 (2005) 7332–7333.
[21] J. Watt, N. Young, S. Haigh, A. Kirkland, R.D. Tilley, Adv. Mater. 21 (2009) 2288–2293.
[22] B. Lim, M. Jiang, P.H.C. Camargo, E.C. Cho, J. Tao, X. Lu, Y. Zhu, Y. Xia, Science 324 (2009) 1302–1305.
[23] M. Hara, U. Linke, Th. Wandlowski, Electrochim. Acta 52 (2007) 5733–5748.
[24] N. Hoshi, K. Kida, M. Nakamura, M. Nakada, K. Osada, J. Phys. Chem. B 110 (2006) 12480–12484.

[25] M. Baldauf, D.M. Kolb, J. Phys. Chem. 100 (1996) 11375–11381.
[26] Z. Huang, X. Liu, K. Li, D. Li, Y. Luo, H. Li, W. Song, L. Chen, Q. Meng, Electrochem. Commun. 9 (2007) 596–598.
[27] T.-C. Wei, C.-C. Wan, Y.-Y. Wang, C.-M. Chen, H.-S. Shiu, J. Phys. Chem. C 111 (2007) 4847–4853.
[28] T. Asano, T. Kubo, Y. Nishikitani, J. Photochem. Photobiol. A-Chem. 164 (2004) 111–115.
[29] W.J. Lee, E. Ramasamy, D.Y. Lee, J.S. Song, Sol. Energy Mater. Sol. Cells 92 (2008) 814–818.
[30] J. Chen, T. Herricks, M. Geissler, Y. Xia, J. Am. Chem. Soc. 126 (2004) 10854–10855.
[31] T. Herricks, J. Chen, Y. Xia, Nano Lett. 4 (2004) 2367–2371.